Solar Energy Materials & Solar Cells 158 (2016) 91–97

Contents lists available at ScienceDirect

Solar Energy Materials & Solar Cells

journal homepage: www.elsevier.com/locate/solmat

Impact of hydrogen on the permanent deactivation of the boron-oxygen-related recombination center in crystalline silicon

Dominic C. Walter [a,*], Jan Schmidt [a,b]

[a] Institute for Solar Energy Research Hamelin (ISFH), Am Ohrberg 1, 31860 Emmerthal, Germany
[b] Department of Solar Energy, Institute of Solid-State Physics, Leibniz Universität Hannover, Appelstr. 2, 30167 Hannover, Germany

ARTICLE INFO

Article history:
Received 24 March 2016
Received in revised form
9 May 2016
Accepted 10 May 2016

Keywords:
Czochralski-grown silicon
Lifetime
Boron-oxygen-related defect
Permanent deactivation

ABSTRACT

In a series of lifetime experiments, we examine the impact of hydrogen on the permanent deactivation of the boron-oxygen (BO)-related defect center in Czochralski-grown boron-doped silicon. In the first experiment, the hydrogen concentration in the external source is varied by the deposition of dielectric layers containing various hydrogen concentrations (aluminum oxide and silicon nitride layers) before applying a fast-firing step at high temperature (> 800 °C). In the second experiment, the sample cooling rate after high-temperature treatment is varied without hydrogen-rich dielectric layer being present and the surface passivation based on aluminum oxide is applied at low temperature afterwards. In both experiments, it is observed that the sample cooling after the high-temperature treatment has the major impact on the dynamics of BO deactivation process and fast cooling rates enable a fast deactivation. No direct impact of the hydrogen content in the dielectric layers being present during the fast-firing step on the dynamics of the BO deactivation is observed. However, the highest lifetimes in excess of 1 ms are only achievable when a hydrogenation step is performed, which we interpret in terms of a hydrogen passivation of background defects of hitherto unknown nature. In a third experiment, we apply an organic passivation layer by spin-coating, which is dried at low temperature (130 °C). We find in this experiment that even without any hydrogen intentionally introduced into the silicon bulk, an effective deactivation of the BO center can be observed, clearly supporting that no hydrogen is required to enable the BO deactivation.

1. Introduction

In boron-doped Czochralski-grown silicon (Cz-Si), the carrier lifetime is limited by a recombination center which is related to a defect complex containing boron and oxygen [1,2]. This BO-related defect reveals its recombination-active properties under illumination at room temperature, leading to a degrading lifetime upon illumination over several hours. This effect is often referred to as light-induced degradation (LID), although the excess electron concentration is actually causing the degradation rather than photons [3]. On the other hand, an annealing step in darkness, e.g. at 200 °C for 10 min, fully recovers the initial lifetime. However, the recovered lifetime, obtained by annealing in darkness, is not stable upon renewed illumination but degrades again towards the degraded lifetime value. The switching between these two states is completely reversible [1]. In 2006, however, Herguth et al. [4] found a loophole to this problem. They showed that the lifetime in boron-doped Cz-Si can be permanently regenerated under illumination or, more precisely, within the presence of excess electrons, at elevated temperature.

In the past, several research groups [5–9] have attributed this permanent regeneration of the lifetime to the presence of hydrogen within the silicon bulk, which was conjectured to be able to passivate the BO defect directly through a hydrogenation of the BO defect. In contrast, Voronkov and Falster [10] proposed a defect model which explained the observed regeneration of the lifetime without any hydrogen being involved. In addition to the fact that the mentioned defect models still contain many speculative elements, it turned out that the distinction between the direct impact of hydrogen in the BO deactivation process or the impact of the high-temperature firing step itself is extremely difficult, as typically hydrogenation is performed during firing. Hence, in this contribution we try to separate the effects of hydrogen and the thermal treatment in order to build the foundations for the development of a new and refined unified defect model.

Three different series of experiments are presented in this contribution, which approach the question from different

* Corresponding author.
E-mail address: d.walter@isfh.de (D.C. Walter).

http://dx.doi.org/10.1016/j.solmat.2016.05.025
0927-0248/

directions. In the first experiment, different passivation schemes via the deposition of dielectric layers which feature very different hydrogen concentrations are applied to the Cz-Si wafers. The impact of the various hydrogen contents after high-temperature firing of the Cz-Si samples on the lifetime is then examined. In the second experiment, the cooling of the lifetime samples after a high-temperature treatment is varied without any hydrogen-rich dielectric layer being present. The surface passivation is carried out after the sample cooling, so that an equally small amount of hydrogen is incorporated into each sample. In the final experiment, a low-temperature passivation (the maximum temperature applied is 130 °C) based on depositing the polymer PEDOT:PSS is applied, which further reduces the in-diffusion of hydrogen from the passivation layer into the silicon bulk. In all experiments, we observe a pronounced permanent recovery of the lifetime upon illumination of our lifetime samples at elevated temperature, demonstrating that the presence of hydrogen in the silicon bulk is not a necessary prerequisite for the BO deactivation.

2. Experimental details

We use wafers from three different boron-doped Cz-grown silicon ingots. The wafers feature base resistivities of $(1.0 \pm 0.03)\,\Omega$ cm, $(1.6 \pm 0.1)\,\Omega$ cm, and $(2.5 \pm 0.1)\,\Omega$ cm determined via four-point-probe measurements and have a final thickness after processing of $(165 \pm 10)\,\mu$m.

Lifetime measurements within this contribution are performed using the Sinton lifetime tester WCT-120. If not mentioned otherwise, the lifetimes are extracted at a fixed injection level of $\Delta n/p_0 = 0.1$, with Δn being the excess electron concentration and p_0 the dark value of the hole concentration, which is in our case identical to the boron concentration, as only non-compensated Cz-Si is used.

3. Experiment #1: impact of dielectric passivation layers with varying hydrogen content

3.1. Sample preparation

Sample processing starts with the removal of the surface damage using a solution of potassium hydroxide (KOH) followed by an RCA cleaning sequence. Afterwards, a phosphorus diffusion is performed at 850 °C for 1:10 h, which results in n^+ layers with a sheet resistance of $(100 \pm 10)\,\Omega/\square$. After the removal of the phosphosilicate glass (PSG) in hydrofluoric acid (HF), the phosphorus-doped regions are removed from both wafer surfaces, again using KOH. In the following, two different surface passivation schemes are applied which feature very different hydrogen concentrations. Within the first sample group, 20 nm Al_2O_3 are deposited on both wafer surfaces via plasma-assisted atomic layer deposition (plasma-ALD) in a FlexAL tool (Oxford Instruments). In the second group, a 10 nm Al_2O_3 layer, also deposited via plasma-ALD, is covered by a 70 nm thick SiN_x ($n = 2.05$) layer deposited via plasma-enhanced chemical vapor deposition (PECVD) using a Roth & Rau SiNA system. Please note that the hydrogen content of the Al_2O_3 and the SiN_x layers differ by about one order of magnitude between 12 and 20 at%[11] for the SiN_x layer and between 1 and 2 at%[12] for the Al_2O_3 layer. After the deposition of the dielectric layers, all samples underwent a fast firing step in a conventional belt-firing furnace (Centrotherm DO-FF-8.600-300) with a set peak temperature of $\vartheta_{Peak} = 850$ °C and various belt speeds between 1.2 m/min and 7.2 m/min. The temperature profiles are measured on identical samples, processed in parallel, using a DATAPAQ Insight Oven Tracker.

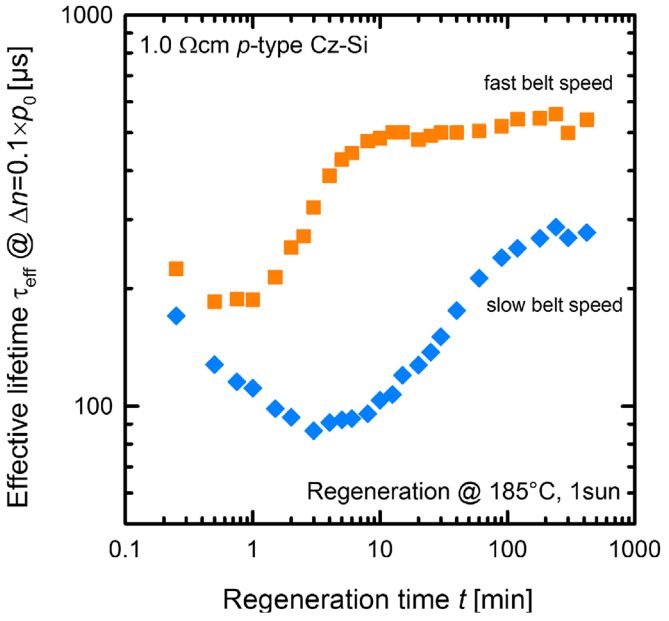

Fig. 1. Regeneration of the effective lifetime τ_{eff} plotted versus the regeneration time t at 185 °C and 100 mW/cm^2 (1 sun) light intensity. A fast belt speed (7.2 m/min, orange squares) leads to a fast regeneration of the lifetime, while for a slow belt speed (1.2 m/min, blue diamonds) a longer regeneration time is needed. (For interpretation of the references to color in this figure legend, the reader is referred to the web version of this article.)

Afterwards, the lifetime measurements are performed and the permanent deactivation of the BO center is performed at a temperature of 185 °C and at various light intensities ranging between 3 mW/cm^2 and 100 mW/cm^2. As illumination source a halogen lamp is chosen. Directly before the permanent deactivation was performed, all samples were annealed at 200 °C for 10 min in darkness.

3.2. Results and discussion

In Fig. 1, the regeneration curves of two lifetime samples passivated with single Al_2O_3 layers and fired at 850 °C set peak temperature with two different belt speeds are displayed. The orange squares correspond to samples fired at a belt speed of 7.2 m/min, while the blue diamonds correspond to a sample fired at a belt speed of only 1.2 m/min. Comparing the saturated lifetimes of the sample treated with the fastest belt speed with the results we obtained recently on various Cz-Si materials with a fired hydrogen-rich dielectric SiN_x layer [13], we find that the saturated lifetime with Al_2O_3 layer is significantly lower compared to that with SiN_x, which were larger than 1 ms. This suggests that the hydrogen-rich layer during the firing is indeed required in order to obtain the very high lifetimes (> 1 ms) we published in [13]. However, we observe the same dynamics for the regeneration process, independent of the hydrogen content in the dielectric passivation layer. As can be seen in Fig. 1, for the fast belt speed, the lifetime clearly regenerates much faster compared to the sample treated with the slow belt speed. In order to evaluate these different regeneration behaviors quantitatively, we extract the recovery rate constants R_{de}.

To determine the recovery rate constants, the measured effective lifetime τ_{eff} is transformed into an effective defect concentration N_t^* using to the equation

$$N_t^* = \frac{1}{\tau_{eff}(t)} - \frac{1}{\tau_0}. \quad (1)$$

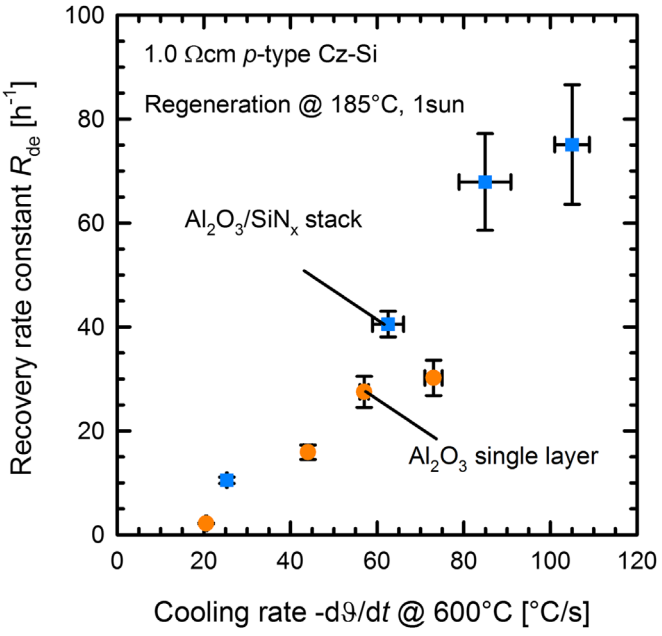

Fig. 2. Recovery rate constant R_{de} plotted versus the cooling rate $-d\vartheta/dt$ at 600 °C after firing. The orange circles correspond to the rate constants determined from the single layer passivated samples, while the blue squares correspond to samples passivated with an Al_2O_3/SiN_x stack, data taken from [14]. (For interpretation of the references to color in this figure legend, the reader is referred to the web version of this article.)

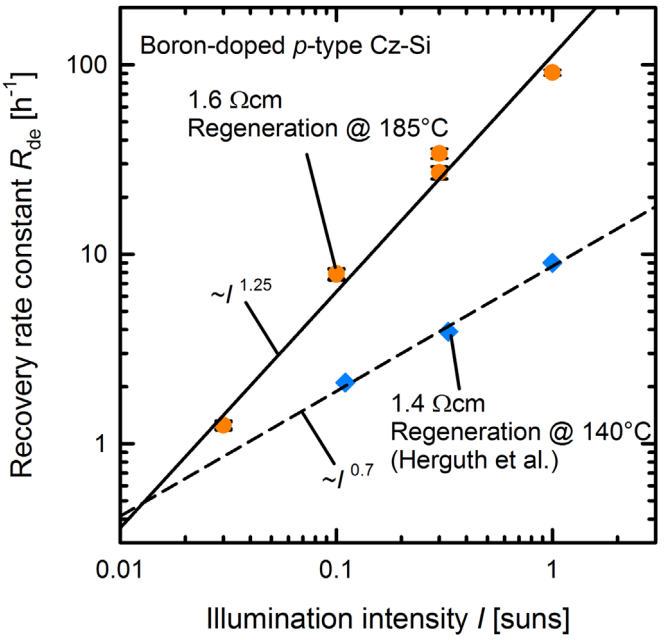

Fig. 3. Recovery rate constant R_{de} plotted versus the illumination intensity I during permanent recovery of lifetime samples with Al_2O_3/SiN_x stack and fired at 7.2 m/min belt speed (orange circles). The regeneration was performed at 185 °C. Blue diamonds correspond to data extracted from Herguth et al. [15] at a temperature of 140 °C from solar cells. The black solid and dashed lines are power law fits. (For interpretation of the references to color in this figure legend, the reader is referred to the web version of this article.)

Here, τ_0 is the lifetime measured after annealing the sample at 200 °C for 10 min in darkness. During the permanent regeneration process, the change of the effective defect concentration can be described by a single exponential function $N_t^* = A \times exp(-R_{de} \times t) + B$, with R_{de} being the recovery rate constant. The rate constant is thus determined from the measured lifetime values by fitting this exponential decay function to our data.

We determine the rate constants R_{de} for all samples treated with different belt speeds and compare the extracted values with the recovery rate constants of samples treated identically which, however, were passivated with an Al_2O_3/SiN_x stack [14]. The result of this comparison is shown in Fig. 2, where the extracted recovery rate constant R_{de} is plotted versus the measured cooling rate $-d\vartheta/dt$ at 600 °C after the firing step at 850 °C. Compared to the samples fired with the Al_2O_3/SiN_x stack, the samples passivated with a single Al_2O_3 layer also show a linearly increasing rate constant with increasing cooling rate after firing. The comparison at equal cooling rates clearly shows that the recovery rate constants R_{de} are quite comparable between the two sample types. The rate constants for the samples with single Al_2O_3 layer tend to be slightly below the R_{de} values determined for the Al_2O_3/SiN_x-passivated samples. However, this can be explained by the two different types of samples, showing completely different reflectivities and hence different excess carrier concentrations at the same illumination intensity (detailed discussion below).

The dependence of the recovery rate constant R_{de} on the illumination intensity I is shown in Fig. 3. The orange symbols correspond to our results obtained on lifetime samples with a base resistivity of (1.6 ± 0.1) Ωcm passivated with Al_2O_3/SiN_x stacks. All of these samples underwent the fast-firing step at 850 °C with a belt speed of 7.2 m/min and were regenerated at 185 °C. The blue diamonds correspond to recovery rate constants extracted by Herguth et al. [15] from solar cells using a regeneration process at 140 °C. In both cases, an increasing rate constant with increasing illumination intensity is observed. From a power law fit to the data, however, different exponents are extracted. For our lifetime data we extract an exponent of (1.25 ± 0.06), while for Herguth's data we extract a value of (0.66 ± 0.06). Despite this difference in the exponents of almost a factor of 2, the general trend is comparable. Note that the recovery of the lifetime at elevated temperatures depends on the concentration of excess carriers, as it was shown in [15]. As with the illumination intensity the concentration of excess carriers increases, the observed trend of an increasing rate constant R_{de} with the increasing illumination intensity I may be expected. However, if results on lifetime samples and solar cells are compared, it has to be taken into account that the change of the excess carrier concentration in the silicon bulk does not only depend on the illumination intensity, but also on the optical properties of the sample and on the overall (injection-dependent) lifetime of the sample during regeneration. Hence, these additional factors might explain the differences observed between the $R_{de}(I)$ dependences of our lifetime samples and the cell results of Herguth et al., shown in Fig. 3.

Coming back to the comparison of the recovery rate constants R_{de} of the samples with different passivation schemes at equal cooling rates shown in Fig. 2, we conjecture that the slight difference between the two sample types in Fig. 2 can be explained by the overall lower excess carrier concentration in the Al_2O_3-passivated Cz-Si samples under the same regeneration conditions as applied on the Al_2O_3/SiN_x-passivated samples. On the one hand the reflectivity considerably varies between the two sample groups. At a wavelength of 1000 nm, which is the dominating wavelength in our halogen lamp spectrum, we calculated the reflectivity of the Al_2O_3-passivated samples to be approximately 32% using the OPAL 2 ray tracer [16]. The reflectivity of the Al_2O_3/SiN_x-passivated samples is only about 13%. On the other hand the

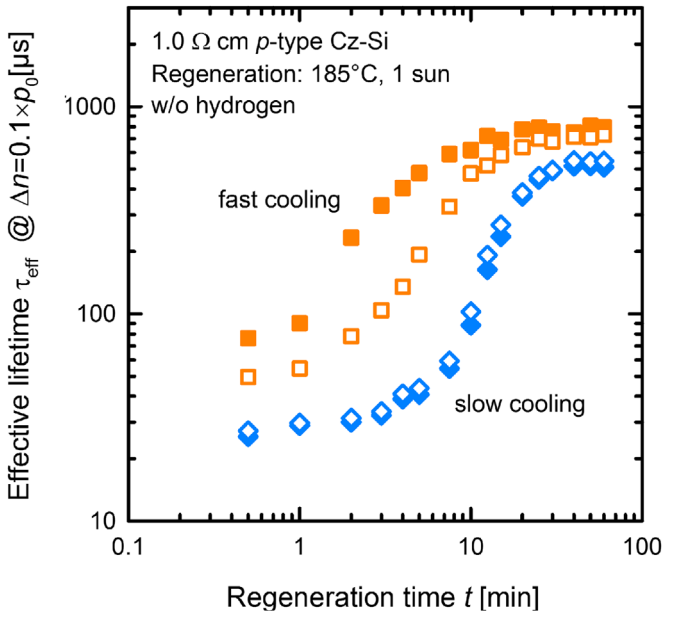

Fig. 4. Effective lifetime τ_{eff} plotted versus the regeneration time t at 185 °C recovery temperature and 100 mW/cm^2 (1 sun) light intensity. Orange squares correspond to samples with a fast cooling after the last high temperature treatment (TD annihilation) at 650 °C, while the blue diamonds correspond to samples with a slow cooling. No hydrogen-containing dielectric layer was present during the high-temperature anneal. (For interpretation of the references to color in this figure legend, the reader is referred to the web version of this article.)

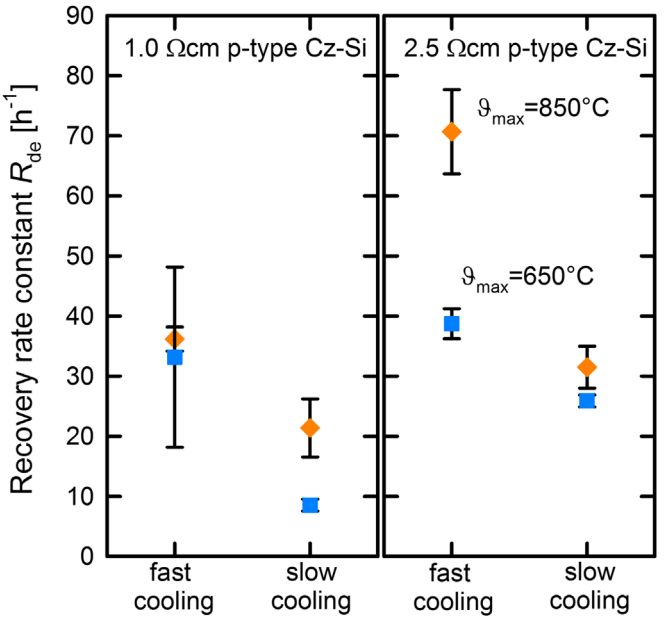

Fig. 5. Recovery rate constant R_{de} for different samples cooled *w/o hydrogen* being present. Two different base resistivities are shown: left 1 Ω cm, right 2.5 Ω cm. Orange diamonds correspond to samples annealed at 850 °C in the last high temperature process, blue squares to samples annealed at 650 °C. (For interpretation of the references to color in this figure legend, the reader is referred to the web version of this article.)

observed lifetime of these sample is significantly lower compared to the samples passivated with the Al_2O_3/SiN_x stack.

Hence, we conclude that the different hydrogen contents in the silicon bulk do not have a major impact on the dynamics of the BO deactivation process.

4. Experiment #2: variation of the sample cooling rate without any hydrogen source present

4.1. Experimental details

In this experiment, the samples were split up into 4 different groups. Groups 1 and 2 underwent a phosphorus diffusion at 850 °C for 0:50 h. Group 1 was removed from the tube furnace at 800 °C, while group 2 remained within the furnace in a nitrogen atmosphere until the furnace was cooled down to 250 °C. In total the cooling down to 250 °C took 215 min Groups 3 and 4 underwent an annihilation step for thermal donors (TDs) in a quartz-tube furnace at 650 °C for 0:30 h in a nitrogen atmosphere. The third group was then removed straight from the tube furnace at 650 °C to realize a high cooling rate, while group 4 remained within the tube furnace until it was cooled down to 250 °C, which took in total 180 min Afterwards, all samples were passivated with Al_2O_3 deposited via thermal ALD in a FlexAL system. The deposition of the Al_2O_3 layers as well as the activation of the passivation layers, performed on a hotplate at ambient air for 15 min, were performed at a maximum temperature of 260 °C. The layer deposition takes 36 min per side.

From literature it is well known that the diffusion of hydrogen in oxygen-rich silicon ($[O_i] \approx 8 \times 10^{17}$ cm^{-3}, which is a typical value for today's Cz-Si) is trap-limited [17,18]. Hence, we must assume that even at deposition times of 1:12 h in total, the diffusion of hydrogen is limited to the first ≈ 20 μm of the silicon bulk [17,19,20]. Because of the trap-limited diffusion of hydrogen, the in-diffusion of hydrogen into the silicon bulk at even lower temperatures (and shorter time spans), e.g. during wet chemical processing, can also be neglected. The permanent deactivation of the BO center was performed at a temperature of 185 °C and a light intensity of 100 mW/cm^2, again using a halogen lamp as light source. Before the permanent deactivation was performed, all samples were illuminated at room temperature for 60 h.

4.2. Results and discussion

In Fig. 4, the dynamics of the BO deactivation in terms of the effective lifetime is shown for four different lifetime samples, which were cooled down rapidly (orange squares) or very slowly (blue diamonds) after the TD annihilation step. During the high-temperature TD annihilation (performed at 650 °C) no dielectric layers were present on the wafer surfaces, i.e. no hydrogen was incorporated into the silicon bulk. As can be seen from Fig. 4, the time span until the lifetime saturates depends critically on the sample cooling, even if there is no hydrogen present during the cooling of the samples. Again, the same trend can be observed: a fast cooling results in a fast recovery of the lifetime, while a slow cooling results in a slow recovery. In Fig. 5, the extracted recovery rate constants R_{de} are shown for different annealing treatments and Cz-Si materials. The orange diamonds correspond to samples annealed at 850 °C, while the blue squares correspond to samples annealed at 650 °C. In all cases, we find a high rate constant for the rapidly cooled samples and a reduced rate constant for samples after a slow cool down. This result further supports our interpretation that the thermal history and especially the cooling of the samples after the last high-temperature step is of major importance for the dynamics of BO deactivation process. Concerning the influence of hydrogen, we would like to point out that the amount of hydrogen introduced into the silicon is extremely small and in particular it is exactly the same for all examined samples within

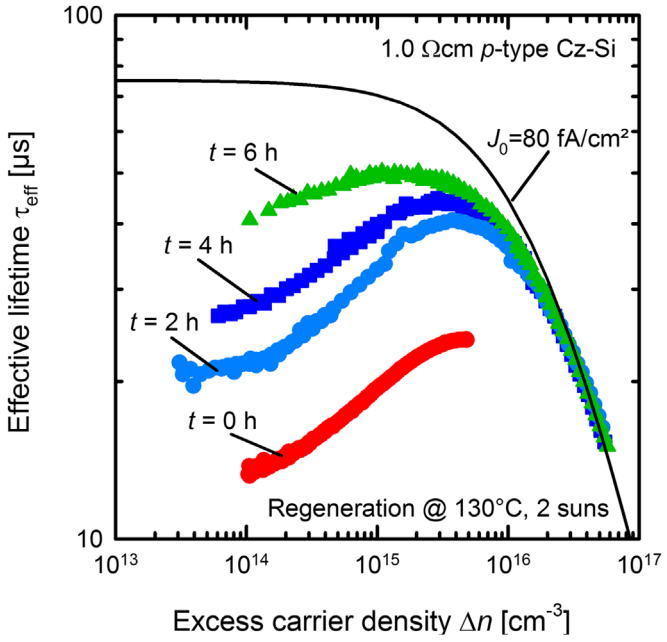

Fig. 6. Injection-dependent carrier lifetime $\tau_{eff}(\Delta n)$ of PEDOT:PSS-passivated samples, exposed between 2 and 6 h to the regeneration conditions at a temperature of 130 °C and 2 suns light intensity. The red curve corresponds to the injection-dependent lifetime before the regeneration process was applied. The black solid line corresponds to the lifetime limited by a saturation current density of J_0=80 fA/cm^2. (For interpretation of the references to color in this figure legend, the reader is referred to the web version of this article.)

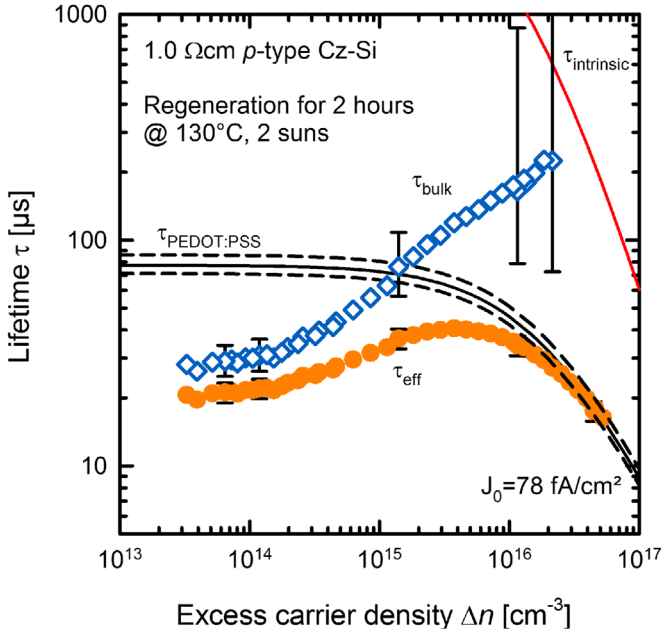

Fig. 7. Bulk lifetime $\tau_b(\Delta n)$, extracted from the measured effective lifetime τ_{eff} and the saturation current density J_0 at the surfaces, for a PEDOT:PSS-passivated sample exposed for 2 h to the regeneration conditions. Orange circles show the measured effective lifetime while the open blue diamonds represent the extracted bulk lifetime. The black solid line is the lifetime limit described by a saturation current density of J_0=78 fA/cm^2. (For interpretation of the references to color in this figure legend, the reader is referred to the web version of this article.)

this experiment, as the same Al_2O_3 surface passivation layer, which was the only source of hydrogen, was applied *after* the last high-temperature treatment. Albeit that, the recovery rate constant varies up to a factor of three between fast and slowly cooled

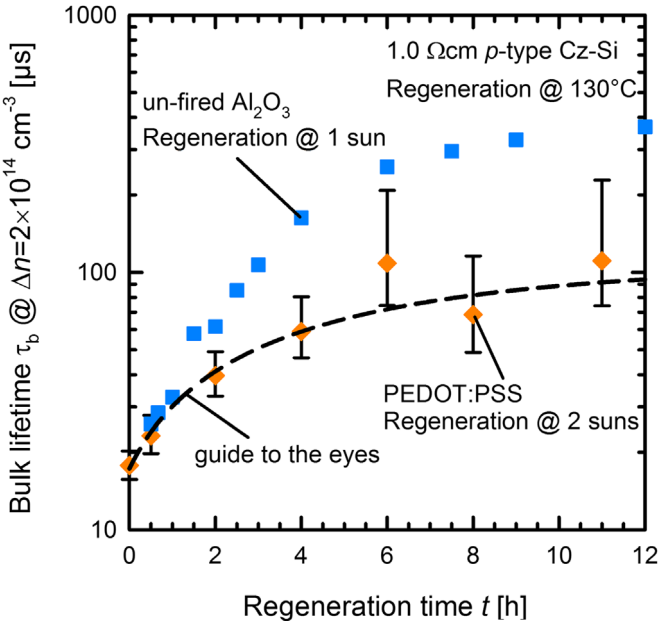

Fig. 8. Bulk lifetime τ_b plotted versus the regeneration time t. The orange diamonds show the increasing lifetimes of the samples passivated with PEDOT:PSS with increasing regeneration time. The black dashed line is a guide to the eyes. For comparison, the effective lifetime τ_{eff} of a sample passivated with Al_2O_3 (blue squares) is also displayed. Both samples regenerate in a comparable time frame of approximately 6 h. (For interpretation of the references to color in this figure legend, the reader is referred to the web version of this article.)

samples, clearly proving that the cooling rate is the most crucial parameter and not the hydrogen content.

5. Experiment #3: polymer-based surface passivation at ultra-low temperatures

5.1. Sample processing

After the removal of the surface damage, a phosphorus diffusion is performed at 850 °C for 1:10 h. After diffusion, the PSG as well as the diffused n^+-regions are removed using HF and KOH, respectively. The surface passivation is then realized by poly(3,4-ethylenedioxythiophene):poly(styrenesulfonate) (PEDOT:PSS) which is deposited using a spin-on technique. PEDOT:PSS is a transparent hole-conducting polymer which allows low saturation current densities of J_0=80 fA/cm^2 [21]. Before PEDOT:PSS deposition, all samples were illuminated at room-temperature. After PEDOT:PSS deposition, the samples are dried on a hotplate at 130 °C for up to 11 h under illumination, using a halogen lamp of approximately 200 mW/cm^2 light intensity. Under these conditions, the PEDOT:PSS is dried and the BO defect is deactivated at the same time.

5.2. Results and discussion

Within this experiment, unfired Cz-Si samples are exposed to the regeneration conditions (in this case 130 °C and 2 suns light intensity) for defined time intervals. In Fig. 6, the injection-dependent lifetimes of four samples are shown which were regenerated for different time intervals. The red curve corresponds to the lifetime before regeneration. The light blue, dark blue and green curves correspond to the lifetime of samples exposed to the regeneration conditions for 2, 4 and 6 h, respectively. While for the red curve the pronounced injection dependence typical of the BO-related defect is observed, the injection dependence weakens with increasing time interval under regeneration conditions. At

increased injection densities ($\Delta n > 10^{16}\,\mathrm{cm}^{-3}$), the lifetime is limited by a saturation current density of $J_0 = 80$ fA/cm^2 provided by the PEDOT:PSS/c-Si interface. This J_0 value is also confirmed by our lifetime measurements on 1.3 Ω cm boron-doped float-zone (FZ) silicon wafers processed in parallel. As the measured effective lifetime of the samples shown in Fig. 6 is strongly influenced by recombination at the surfaces, we extract the bulk lifetime τ_b of the Cz-Si material by determining the saturation current density J_0 of the PEDOT:PSS/c-Si interface in the high-injection regime and subtracting its influence from the measured effective lifetime τ_{eff} using the equation:

$$\tau_b(\Delta n) = \left(\frac{1}{\tau_{eff}(\Delta n)} - \frac{2 \times J_0 (p_0 + \Delta n)}{q n_i^2 W} \right)^{-1}, \quad (2)$$

with q being the elementary charge, n_i the intrinsic carrier concentration and W the sample thickness. Please note that this equation only holds if the injection dependence of the PEDOT:PSS surface passivation can indeed be expressed by a single J_0 value, which will be assumed in the following. From the lifetime measurements on our FZ reference samples we know that this is a reasonable assumption. However, even if the assumption does not hold, the extracted bulk lifetimes can be considered as a lower limit for the actual bulk lifetime. In Fig. 7, an example for the extraction of the bulk lifetime τ_b from the measured effective lifetime τ_{eff} for a Cz-Si sample exposed for 2 h to the regeneration conditions is displayed. At low-injection levels, $\Delta n < 5 \times 10^{14}\,\mathrm{cm}^{-3}$, the bulk lifetime can be determined quite accurately. However, at higher injection conditions ($\Delta n > 10^{15}\,\mathrm{cm}^{-3}$), the uncertainty in the extracted τ_b is larger compared to the determined bulk lifetime itself. In the following, we perform this analysis for all investigated time spans and extract the bulk lifetimes in the low-injection regime at a fixed injection density of $\Delta n = 2 \times 10^{14}\mathrm{cm}^{-3}$. The result of this analysis is shown in Fig. 8 where the extracted bulk lifetime τ_b is plotted versus the regeneration time t. As can be seen by the black dashed line (guide to the eyes), the bulk lifetime clearly increases with regeneration time. Moreover, the recovery of the lifetime proceeds in a time frame which is comparable to the recovery time of a sample passivated with a single Al_2O_3 layer (blue squares), deactivated at a temperature of 130 °C and a light intensity of 100 mW/cm^2. Despite the strong scatter in the data obtained from the samples passivated with PEDOT:PSS, the lifetime seems to saturate after 6 h, faster than the sample passivated with Al_2O_3. This difference might be attributed, at least partially, to the increased light intensity (200 mW/cm^2) during regeneration of the PEDOT:PSS passivated sample.

This result further supports that the deactivation of the BO defect does not require hydrogen. Especially, a fast-firing step with a hydrogen-rich dielectric layer is not required for the BO deactivation. Hence, we conclude from our experiments that hydrogen is not a necessary prerequisite for the BO deactivation. Future BO defect models should hence not rely on the presence of hydrogen in the silicon bulk during permanent deactivation.

6. Summary

We have presented three different experiments with the intention to separate the effects of hydrogen and thermal history on the dynamics of the permanent deactivation of boron-oxygen-related recombination centers in crystalline silicon.

In the first experiment, we have shown that the regeneration dynamics of the lifetime under illumination at elevated temperatures is not affected by different hydrogen contents in the dielectric layers, deposited onto the sample surfaces prior to a high-temperature fast-firing process. Even if the surface passivation was performed after the fast-firing step, equal recovery rate constants are observed. However, omitting any hydrogenation (via fast-firing with a hydrogen-rich dielectric layer being present) we were not able to achieve lifetimes in excess of 1 ms. We interpret this result in terms of an effective hydrogen passivation of background defects of yet unidentified nature.

In the second experiment, we have examined the influence of sample cooling after the last high-temperature treatment without the presence of hydrogen. A surface passivation based on Al_2O_3 at a maximum temperature of 260 °C was deposited onto the surfaces only after the high-temperature step. The experimental results clearly revealed the crucial importance of the sample cooling on the dynamics of the regeneration process. Moreover, even with exactly the same, very low hydrogen content in the silicon bulk, we have observed a pronounced regeneration of the lifetime in all cases with the dynamics depending on the sample cooling only.

In the third experiment, we have shown that a pronounced permanent recovery of the lifetime is observed even without any hydrogen in-diffusion into the silicon bulk. This result is based on a low-temperature (maximum temperature 130 °C) surface passivation using the polymer PEDOT:PSS.

In summary, the results of our experiments clearly prove that hydrogen introduced from dielectric layers present during high-temperature treatments is not responsible for the observed permanent regeneration of the lifetime in boron-doped Czochralski-grown silicon upon illumination at elevated temperature. However, in order to obtain very high lifetimes in excess of 1 ms, a hydrogen-rich dielectric layer as well as a fast-firing step is required, which we attribute to the hydrogen passivation of background defects of hitherto unknown nature.

Acknowledgement

The authors would like to thank R. Falster, V. Voronkov (both SunEdison) and B. Lim (now with SERIS) for many fruitful discussions, and the State of Lower Saxony for funding.

References

[1] J. Schmidt, A.G. Aberle, R. Hezel, Investigation of carrier lifetime instabilities in Cz-grown silicon, in: Proceedings 26th IEEE PVSC, Anaheim, CA (IEEE, New York, 1997), 1997, p. 13.
[2] S.W. Glunz, S. Rein, W. Warta, J. Knobloch, W. Wettling, On the degradation of Cz-Silicon solar cells, in: Proceedings of the 2nd WC-PVSEC, Vienna, Austria (WIP, Munich, 1998), 1998, p. 1343.
[3] K. Bothe, J. Schmidt, Fast-forming boron-oxygen-related recombination center in crystalline silicon, Appl. Phys. Lett. 87 (2005) 262108.
[4] A. Herguth, G. Schubert, M. Kaes, G. Hahn, A new approach to prevent the negative impact of the metastable defect in boron doped Cz silicon solar cells, in: Proceedings of the 32nd IEEE PVSC (4th WCPEC), Waikoloa, USA, 2006, pp.940–943.
[5] K.A. Münzer, Hydrogenated silicon nitride for regeneration of light induced degradation, in: Proceedings of the 24th EUPVSEC Hamburg, 2009, pp. 1558–1561.
[6] S. Wilking, A. Herguth, G. Hahn, Influence of hydrogen on the regeneration of boron-oxygen related defects in crystalline silicon, J. Appl. Phys. 113 (2013) 194503.
[7] B.J. Hallam, S.R. Wenham, P.G. Hamer, M.D. Abbott, A. Sugianto, C.E. Chan, A. M. Wenham, M.G. Eadie, G. Xu, Hydrogen passivation of B-O defects in Czochralski silicon, Energy Procedia 38 (2013) 561–570.
[8] N. Nampalli, B. Hallam, C. Chan, M. Abbott, S. Wenham, Evidence for the role of hydrogen in the stabilization of minority carrier lifetime in boron-doped Czochralski silicon, Appl. Phys. Lett. 106 (2015).
[9] N. Nampalli, B.J. Hallam, C.E. Chan, M.D. Abbott, S.R. Wenham, Influence of Hydrogen on the mechanism of permanent passivation of boron-oxygen defects in p-type Czochralski silicon, IEEE J. Photovolt. 5 (2015) 1580–1585.
[10] V.V. Voronkov, R. Falster, Light-Induced boron-oxygen recombination centres in silicon: understanding their formation and elimination, Solid State Phenom. 205–206 (2013) 3–14.

[11] B. Lenkeit, Elektronische und strukturelle Eigenschaften von Plasma-Siliziumnitrid zur Oberflächenpassivierung von siebgedruckten, bifacialen Silizium-Solarzellen (Ph.D.), Hannover, Germany, 2002.
[12] B. Hoex, J. Schmidt, P. Pohl, M.C.M. van de Sanden, W.M.M. Kessels, Silicon surface passivation by atomic layer deposited Al_2O_3, J. Appl. Phys. 104 (2008) 44903.
[13] D.C. Walter, B. Lim, J. Schmidt, Realistic efficiency potential of next-generation industrial Czochralski-grown silicon solar cells after deactivation of the boron–oxygen-related defect center, Progress Photovolt.: Res. Appl. (2016) n/a–n/a.
[14] D.C. Walter, B. Lim, K. Bothe, V.V. Voronkov, R. Falster, J. Schmidt, Effect of rapid thermal annealing on recombination centres in boron-doped Czochralski-grown silicon, Appl. Phys. Lett. 104 (2014) 42111.
[15] A. Herguth, G. Schubert, M. Kaes, G. Hahn, Further investigations on the avoidance of boron-oxygen related degradation by means of regeneration, in: Proceedings of the 22nd EUPVSEC, Milan, Italy, 2007, pp. 893–896.
[16] K.R. McIntosh, S.C. Baker-Finch, OPAL 2: Rapid optical simulation of silicon solar cells, in: Proceedings of the 38th IEEE PVSC, Austin, Texas, 2012, pp. 265–271.
[17] Y.L. Huang, Y. Ma, R. Job, A.G. Ulyashin, Hydrogen diffusion at moderate temperatures in p-type Czochralski silicon, J. Appl. Phys. 96 (2004) 7080–7086.
[18] S. Kleekajai, F. Jiang, M. Stavola, V. Yelundur, K. Nakayashiki, A. Rohatgi, G. Hahn, S. Seren, J. Kalejs, Concentration and penetration depth of H introduced into crystalline Si by hydrogenation methods used to fabricate solar cells, J. Appl. Phys. 100 (2006).
[19] A. Mogro-Campero, Drastic changes in the electrical resistance of gold-doped silicon produced by a hydrogen plasma, J. Electrochem. Soc. 132 (1985) 2006.
[20] R.C. Newman, J.H. Tucker, A.R. Brown, S.A. McQuaid, Hydrogen diffusion and the catalysis of enhanced oxygen diffusion in silicon at temperatures below 500 °C, J. Appl. Phys. 70 (1991) 3061.
[21] J. Schmidt, V. Titova, D. Zielke, Organic-silicon heterojunction solar cells: open-circuit voltage potential and stability, Appl. Phys. Lett. 103 (2013) 183901.